# Magnet deviation measurements and their consideration in electromagnetic field simulation

Peter Offermann*, Isabel Coenen*, David Franck* and Kay Hameyer*

*Institute of Electrical Machines
RWTH Aachen University
Schinkelstrasse 4
D-52062 Aachen, Germany
E-mail: Peter.Offermann@IEM.rwth-aachen.de

***Abstract*—Due to their manufacturing process arc segment magnets for the use in permanent-magnet synchronous machines (PMSM) may show deviations from their intended ideal magnetization. Using magnets with unfavourable error constellations in one rotor of a PMSM will result in a spatial unsymmetric air gap field, causing undesired parasitic effects as e.g. torque pulsations. Most manufacturer information only contain the mean values of the magnetization as well as certain guaranteed error bounds, not stating if (and how) the magnetization will vary spatial over a set of magnets. In order to allow an accurate consideration of these deviations in the machine simulation, the emitted radial field of a set of magnets has been measured and compared to their assumed magnetisation using finite element method (FEM). As a result, the measured deviations can be quantified and the influence of magnet deviations can be estimated using e.g. stochastic collocation methods in combination with the FEM.**

***Index Terms*—finite element method, magnetization errors, measurements, stochastics variations**

## I. Introduction

The simulation of an electrical machine employing the finite element method (FEM) requires the exact knowledge of the machine's geometry, its excitations and its material properties. For machines which are manufactured in mass production, the material or geometry of one specific instance of the designed machine may vary from its specified targets [1], leading in the worst case to a non-fulfilment of the rated machine's data.

For geometry variations a typical cause is the abrasion of the punching tools. Varying material properties may be caused e.g. by a stochastic jitter in the orientation of the punched stator lamination sheets, which can be tainted with anisotropy. Causes for variations in excitations can either arise from the converter or – in case of a permanent-magnet synchronous machines (PMSM) – from magnet deviations [2] with respect to their intended ideal magnetization [3]. Using magnets with unfavourable error constellations in one rotor of a PMSM will result in a spatial unsymmetric air gap field, causing undesired parasitic effects as torque pulsation [4], [5].

Most manufacturer information only contain the mean values of the magnetization as well as certain guaranteed error bounds, not stating if (and how) the magnetization will vary spatial over a set of magnets. The goal of this publication hence is to improve the simulation of electrical machines by reducing the described epistemic uncertainty of magnet variations. Therefore, a magnet test-bench has been created, in order to measure the emitted radial field of a set of magnets. From this, the modality and probability distribution of the occurring variations have been deduced.

The comparison of the magnets' FEM-simulations with their measurements may allow the calculation of improved simulation parameters for complete machine simulations. For the measured magnets, which were diametrally magnetized, three error-types have been identified: A general variation of the flux-density's strength of up to 11.6%, a maximal local, angle deviation at the magnet's outer borders of 8° and local errors of up to 9.1%.

## II. Magnetization measurement test-bench

In order to obtain reliable data about possible magnetisation errors, a test bench for the evaluation of surface magnets has been built. In the following the sensor selection (sec. II-A) and the test-bench construction (sec. II-B) are described.

### A. Sensor selection

Typical methods to measure the magnetic flux-density are Hall-sensors and Helmholtz-coils. In this paper, a Hall-sensor as depicted in fig. 1 has been selected, due to the following reasoning:

For best results, both methods require that the measured magnetic field is oriented perpendicular to the measuring coil respectively Hall-sensor. This can be easier accomplished for larger sensors than for very small

devices. Hall-sensors can be miniaturized due to the fact that an interaction with a given current is measured. Therefore the concomitant reduction of the Hall-constant $C_H$, being a consequence of a reduction in material volume, can be compensated to certain extents with an increase in the measurement current (fig. 1). This allows to measure field components nearly pointwise.

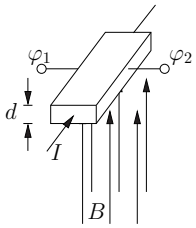


Fig. 1. Hall-sensor and its distinctive input sizes.

Helmholtz-coil configurations – in contrast to Hall-sensors – always measure the the overall magnetic flux-density. Due to this integration over the magnet's surface flux-density, however, a pointwise selective resolution of the magnetic field is no longer possible. Global angle offsets in the magnetization can be detected with both measurement methods by either using multiple sensors respectively coils or by turning the magnet under test. For this purpose, coils are preferable, because their orientation is better adjustable and an integration over all local values for a single angle value is implemented intrinsic in the coil. Local angle errors however cannot be detected using such a setup. Lastly, coil measurements are less noise sensitive because the integration already smoothes some measurement noise.

The decisive factor for Hall-sensors was the interest in local magnet variations, since most publications until now focus only on global magnet variations [6], [7] in electrical machines. Furthermore, this selection allows the analysis of possible locational misalignments of the magnets and will enable a later use of the measured variations in conformal mapping Ansatz functions [8], [9].

### *B. Test-bench construction*

For the construction of the magnet test bench, Hall-sensors of the type *HE-244* [10] were selected. Table II-B summarizes the main features of the selected sensor:

TABLE I
PROPERTIES OF THE USED HALL SENSOR.

| | **value** | **unit** |
|---|---|---|
| **supply current** | up to 10 | mA |
| **sensitivity** | 90 to 190 | V / (A · T) |
| **linearity hall voltage** | typical $\leq 0.2$ | % |

Three sensors for the measurement of the magnetic field components $B_x$, $B_y$ and $B_z$ are located on an index arm with predefined 90 degree edges, in order to achieve a good positioning. The sensors are positioned directly on adjacent edges to measure the field at approximately one point as depicted in fig. 2.

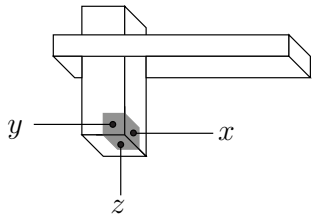


Fig. 2. Positions and labelling of the used Hall-sensors on the measurement anchor.

The index arm itself is mounted on a gibbet, which is constructed in such a way, that it allows a position adjustment in all three dimensions. Below the index arm the magnets under test can be mounted upon a cylindric shaft which rotates around its symmetry-axis (fig. 3, 4).

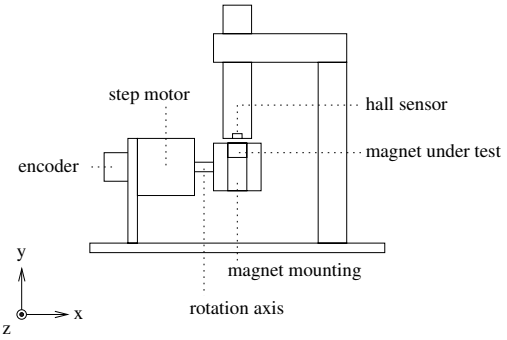


Fig. 3. Schematic scetch of the created test bench for magnet measurements.

This allows the use of a connected stepper-motor to measure the field along a circular line over the magnet's surface. To avoid field distortion by flux guidance all relevant test bench components have been constructed from aluminium. Data acquisition and the stepper-motor control are implemented using a *dSpace*-system in combination with a PC.

## III. RESULTS

In this study 52 magnets with diametral magnetization and a field strength of $B_r = 1.04T$ were analysed, consisting of two equally sized groups with either north- or south-pole on the outer magnet circumference. For each magnet, the Hall-voltage of the radial outwards pointing flux-density was measured 1.5mm above the magnet's surface. The magnet's dimensions are given in fig. 5.

### *A. Simulations*

In the simulations, the magnet (as depicted in fig. 5) is surrounded by an air layer which measures ten times

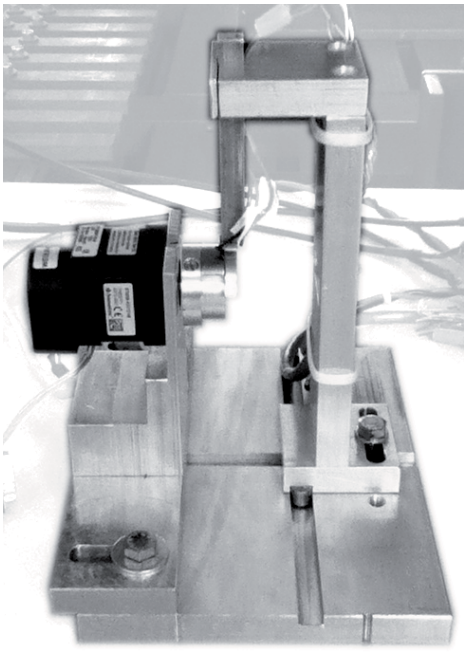

Fig. 4. Photograph of the constructed magnet test bench.

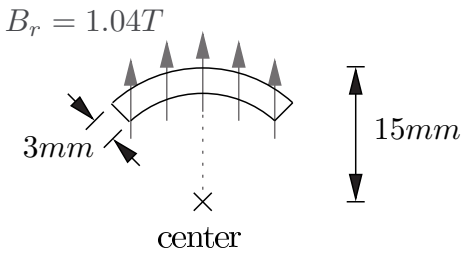


Fig. 5. Dimensions of the measured magnets.

the magnet's height in every direction [11]. The applied solver implements the magnetic vector-potential formulation. All boundaries were set as Neumann conditions. The radial flux-density was sampled along a circumference of 1.5mm above the magnet.

### *B. Measurements*

*1) Repetition measurements:*
Repetitive measurements were executed to determine the test-bench's measurement reproducibility. The average error between two arbitrary measurements of the same magnet is below 0.5% and mainly caused by very small positioning errors of the magnet in the tangential direction of the measurement shaft. Fig. 6 depicts five repetitive measurements of magnet #7.

*2) Post-processing of measurements:*
For data acquisition, every magnet is inserted, measured, and removed from the test-bench five times (fig. 6). Afterwards, the repetitive data of each magnet data are scanned for obvious misplacement errors. If they exist, the worst deviating measurement is removed. Thereafter,

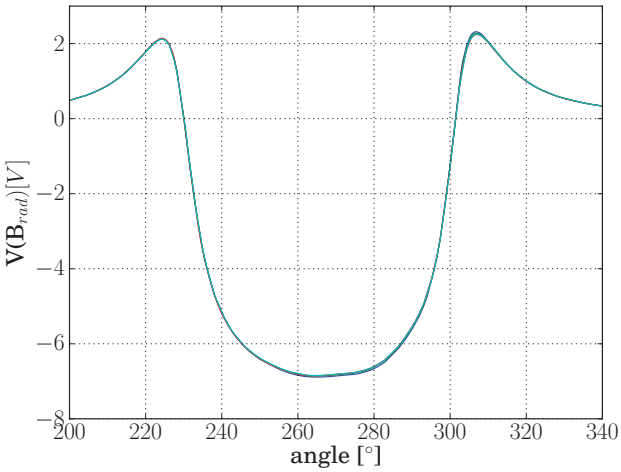


Fig. 6. Five repetitive measurements of magnet #7, showing the test-bench's reproduction quality.

the repetitive measurements are aligned to have their outer minima centred at around fixed value. Ultimately, the remaining, centred flux-density values of the magnet are averaged. Fig. 7 shows – for the purpose of demonstration exaggerated – examples of the described process.

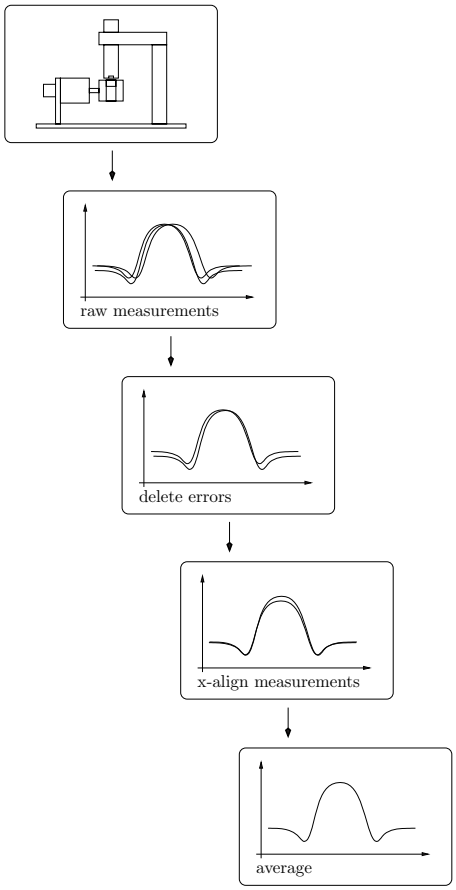


Fig. 7. Post-processing of measured flux-density curves.

*3) Variation measurements:*
Figure 8 presents the results of the variation measure-

ments for all magnets which have their north pole located on the outer side. Two obvious variations can be directly identified:

- Strength variations in the overall remanence flux-density per magnet,
- Strong deformations from the expected curve shape in terms of local variations.

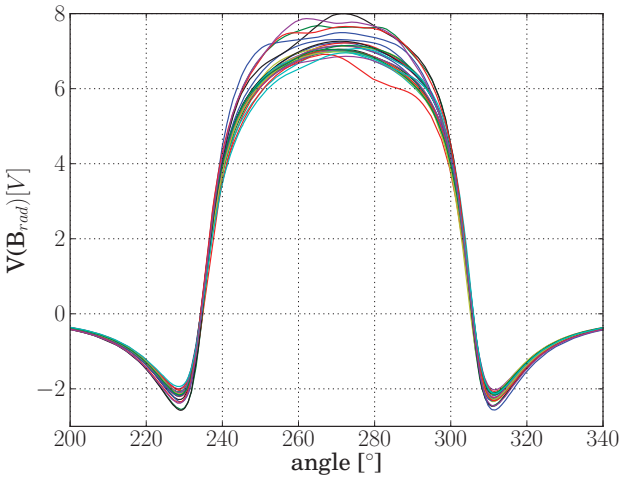


Fig. 8. Measured radial flux-density 1.5mm above each magnet's centre in the magnet group 'north-up'.

Fig. 9 shows accordingly the likelihood of occurrence for the radial outwards pointing flux-density over the magnet angle for the opposite magnet group. Due to the envelope shape of the resulting curve, the strong influence of the variations is even more obvious.

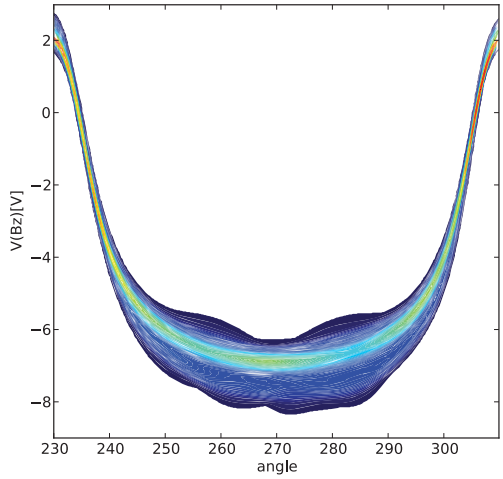


Fig. 9. Probability of measured magnetisation strength, probabilities ranging from low (dark) to high (light).

### C. Comparison of measurements and simulations

In order to quantify the strength of the occurring deviations in terms of changes in excitation (in contrast to changes in the resulting flux-density), the excitation of each magnet had to be reconstructed from the given measurements. To solve this inverse problem [12], a straightforward approach was to compare the measured radial flux-density component of each magnet to a set of simulations. In these simulations, the magnet's remanence flux-density $B_r$ was varied as parameter $\xi_1$, applying the simulation conditions presented in section III-A. However, the resulting shapes did not agree to the measured curves. The employed magnetisation model was therefore extended to include a second deviation parameter $\xi_2$, allowing an angle spread in magnetisation as given in fig. 10 and yealding the excitation given in eq. 1:

$$\vec{B}(\Delta\alpha, \xi_1, \xi_2) = B_r(\xi_1) \cdot \begin{pmatrix} \cos(\alpha_{mid} + \Delta\alpha(\xi_2)) \\ \sin(\alpha_{mid} + \Delta\alpha(\xi_2)) \\ 0 \end{pmatrix} \quad (1)$$

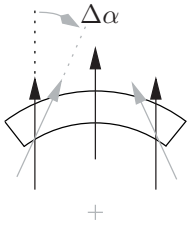


Fig. 10. Determined second deviation parameter $\xi_2$ (grey) from the ideal, unidirectional magnetisation.

Applying both variation types, the magnet excitation parameters could be reconstructed sufficiently in most cases using the least-square minimization from eq. 2 for parameter determination:

$$\min_{\xi_1,\xi_2} \left| \sum_{\alpha=230°}^{310°} \left[ B_{rad,sim}(\alpha, \xi_1, \xi_2) - B_{rad,mes}(\alpha) \right]^2 \right| \quad (2)$$

Fig. 11 shows the comparison of the measured radial flux-density (dashed) in comparison to the best fitting simulated curve (solid). The divergence of both curves at

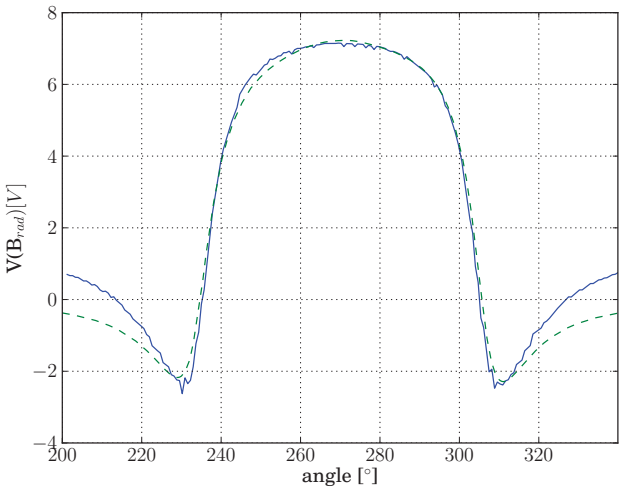


Fig. 11. Measured (dashed) radial outwards pointing flux-density in comparison to its best fitting siumlation for magnet #1.

the outer side of both graphs can safely be neglected here, because they are caused by effects of the 2D-simulation and are considered as not relevant, as this area is not above, but beside the magnet.

Figure 12 finally shows the comparison of measured and simulated radial outwards pointing flux-density for a magnet having a local magnetisation error. As the graph clearly shows, this behaviour cannot be reproduced by the applied model yet. The three identified error-types finally have been identified to: flux-density's strength variations of up to 11.6%, a maximal local, angle deviation at the magnet's outer borders of 8° and local errors of up to 9.1%

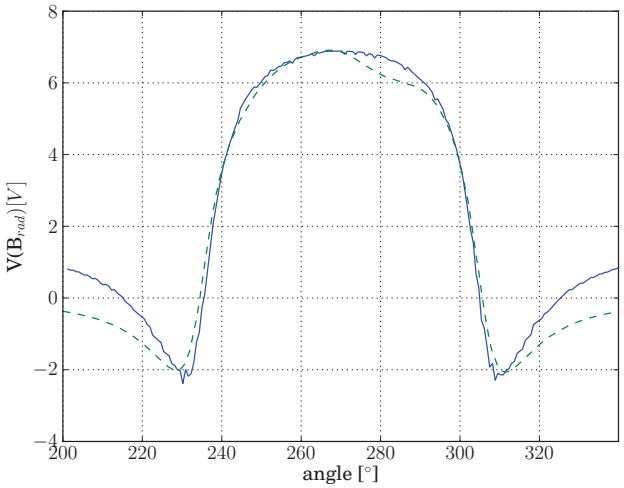


Fig. 12. Measured (dashed) radial outwards pointing flux-density in comparison to its best fitting siumlation for magnet #13. Local errors cannot be reproduced yet.

## IV. Conclusions

The presented methodology allows an accurate determination of remanence flux-density variations above the surface of a set of magnets or rotors. A comparison of the measured curves with the magnet's simulated and intended remanence flux-density reveals, in which way the used FE-magnet-models have to be adopted to be used in stochastic considerations of parameter variations in electrical machines. Necessary implementations are a scalable magnetization strength and an over the magnet changing deviation angle. Optional, local errors can be considered as well. The resulting magnet parameters finally can be used for uncertainty propagation applying appropriate tools as stochastic collocation [13] or polynomial chaos approaches [14] to propagate the magnet deviations onto output sizes of interest.

## V. Acknowledgement

The results presented in this paper have been developed in the research project Propagation of uncertainties across electromagnetic models granted by the Deutsche Forschungsgemeinschaft (DFG).

## References

[1] M. Cioffi, A. Formisano, and R. Martone, "Stochastic handling of tolerances in robust magnets design," *IEEE Transactions on Magnetics*, vol. 40, no. 2, pp. 1252 – 1255, march 2004.

[2] M.-F. Hsieh, C.-K. Lin, D. Dorrell, and P. Wung, "Modeling and effects of in-situ magnetization of isotropic ferrite magnet motors," in *Energy Conversion Congress and Exposition (ECCE), 2011 IEEE*, sept. 2011, pp. 3278 –3284.

[3] K.-C. Kim, S.-B. Lim, D.-H. Koo, and J. Lee, "The shape design of permanent magnet for permanent magnet synchronous motor considering partial demagnetization," *IEEE Transactions on Magnetics*, vol. 42, no. 10, pp. 3485 –3487, oct. 2006.

[4] D. Torregrossa, A. Khoobroo, and B. Fahimi, "Prediction of acoustic noise and torque pulsation in pm synchronous machines with static eccentricity and partial demagnetization using field reconstruction method," *IEEE Transactions on Industrial Electronics*, vol. 59, no. 2, pp. 934 –944, feb. 2012.

[5] G. Heins, T. Brown, and M. Thiele, "Statistical analysis of the effect of magnet placement on cogging torque in fractional pitch permanent magnet motors," *IEEE Transactions on Magnetics*, vol. 47, no. 8, pp. 2142 –2148, aug. 2011.

[6] F. Jurisch, "Production process based deviations in the orientation of anisotropic permanent magnets and their effects onto the operation performance of electrical machines and magnetic sensors – german –," *International ETG-Kontress Tagungsband, (ETG-FB 107)*, no. 1, pp. 255–261, 2007.

[7] I. Coenen, M. Herranz Gracia, and K. Hameyer, "Influence and evaluation of non-ideal manufacturing process on the cogging torque of a permanent magnet excited synchronous machine," *COMPEL*, vol. 30, no. 3, pp. 876–884, 2011.

[8] M. Hafner, D. Franck, and K. Hameyer, "Accounting for saturation in conformal mapping modeling of a permanent magnet synchronous machine," *COMPEL*, vol. 30, no. 3, pp. 916–928, May 2011.

[9] D. Zarko, D. Ban, and T. Lipo, "Analytical calculation of magnetic field distribution in the slotted air gap of a surface permanent-magnet motor using complex relative air-gap permeance," *Magnetics, IEEE Transactions on*, vol. 42, no. 7, pp. 1828 – 1837, july 2006.

[10] H. Electronics, "He244 series analog hall sensor - datasheet," Download from www.hoeben.com, downloaded at 15.08.2012, November 2011.

[11] P. Offermann and K. Hameyer, "Non-Linear stochastic variations in a magnet evaluated with Monte-Carlo simulation and a polynomial Chaos META-Model," in *XXII Symposium on Electromagnetic Phenomena in Nonlinear Circuits,EPNC 2012*. Pula, Croatia: PTETIS Publishers, June 2012, pp. 21–22.

[12] A. Mohamed Abouelyazied Abdallh, "An inverse problem based methodology with uncertainty analysis for the identification of magnetic material characteristics of electromagnetic devices," Ph.D. dissertation, Ghent University, 2012.

[13] E. Rosseel, H. De Gersem, and S. Vandewalle, "Nonlinear stochastic Galerkin and collocation methods: application to a ferromagnetic cylinder rotating at high speed," *Communications in Computational Physics*, vol. 8, no. 5, pp. 947–975, 2010.

[14] B. Sudret, "Uncertainty propagation and sensitivity analysis in mechanical modesl – contributions to structural reliability and stochastic spectral methods," Ph.D. dissertation, Universite BLAISE PASCAL - Clermont II, Ecole Doctorale Sciences pour l'Ingenieur, 2007.